

# An Integrated Scheme for Machine Hysteresis Loss Evaluations based on Iterative Magnetic Equivalent Circuits and Emulated Epstein Frame Tests

Cheng-Tsung Liu<sup>1</sup>, Hsiu-Ying Lin<sup>1</sup>, and Chang-Chou Hwang<sup>2</sup>

<sup>1</sup>Department of Electrical Engineering, National Sun Yat-Sen University, 70, Lien-Hai Road, Kaohsiung, 804, Taiwan

<sup>2</sup>Department of Electrical Engineering, Feng Chia University, 100, Wen-Hua Road, Taichung, 407, Taiwan

<sup>1</sup>ctliu@ieee.org, <sup>2</sup>cchwang@fcu.edu.tw

**Abstract** — An iterative scheme that can adequately integrate the nonlinear magnetization properties of isotropic magnetic steels and a nodal-based equivalent magnetic network is provided, such that the flux densities inside an electric machine can be systematically evaluated. Based on the time-domain fluxes and an emulated Epstein Frame test circuit, the required magnetization inputs for performing the numerical tests at all the nodal regions can be devised. Thus the detailed hysteresis inner-loop characteristics resulted from machine structures and magnetization harmonics can be properly modeled, and the corresponding hysteresis losses can be calculated by assembling the individual ones from all the regions. Confirmed by 3-D finite element analyses, it is clear that a satisfactory machine hysteresis loss evaluation scheme, by considering the possible magnetic nonlinearity and harmonic effects, can be established.

## I. INTRODUCTION

With the ever increasing operational efficiency requirements and magnetization complexities, selections of appropriate magnetic steels for constructing electric machines have now become important factors to meet the energy saving and performance enhancement objectives. Aside from the cost concerns, proper iron loss evaluations of the machines with different magnetic steels will be the key issue. However, unless the evaluated results are obtained by detailed finite element analyses (FEA) on the specific machine structures, large discrepancies are inevitably exhibited among those obtained from steel manufacturers' datasheets and the physical measured ones. A systematic scheme that can evaluate the machine hysteresis losses with less computation efforts than the FEA and still provide reasonable enough accuracies is certainly desired by both the steel manufacturers and the machine producers [1], [2].

## II. THE PROPOSED INTEGRATED ITERATIVE SCHEME

Based on proper analytical derivations [3], [4], the air-gap flux density distributions of specific machines can be conveniently modeled. However, by taking the China Steel Corporation (CSC) 50CS470 magnetic steel as an example, with its nonlinear magnetizing characteristics being illustrated in Fig. 1, it is clear that those analytical air-gap flux modeling schemes can not be directly applied for evaluating those flux information in the machine cores. By introducing the common magnetic equivalent circuit (MEC) concept [5], [6] and using the devised air-gap flux density information, as illustrated in Fig. 2, an iteratively-modified permeance matrix will be established based on the nodal magnetomotive force (MMF) information and the magnetizing characteristics of the core steels. From the converged solutions, the operational fluxes in all the given magnetic regions inside the machine core can be

estimated. Hence the corresponding machine hysteresis losses can be assembled by integrating the individual flux density  $B_{mj}$  and magnetic field intensity  $H_{mj}$  information on those regions together as:

$$P_h = \sum_j P_{hj} = \sum_j \left( \oint H_{mj} dB_{mj} \right) \times f / D, \quad (1)$$

where  $f$  is the operational frequency and  $D$  is the steel density.

It is clear that the above general expression for hysteresis loss evaluations can only provide averaged results with specified frequency levels. To cover the effects of operational harmonics and recoil magnetizations, as shown in Fig. 3, an equivalent circuit that can emulate the standard Epstein Frame test is adopted [7], [8]. Though many numerical models have been developed for representing the nonlinear characteristics

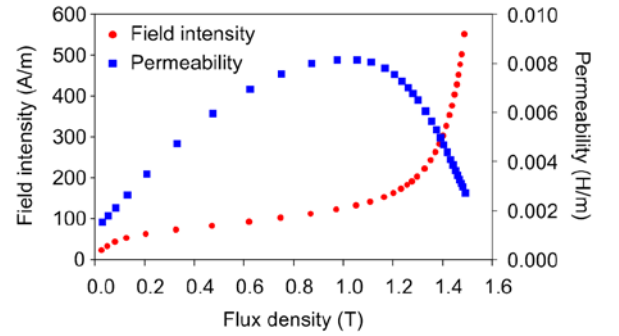


Fig. 1. Magnetizing characteristics of the CSC 50CS470 magnetic steel.

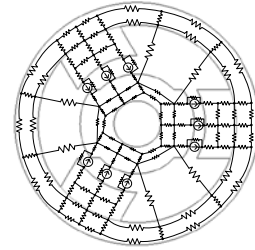


Fig. 2. Conceptual illustration of the magnetic equivalent circuit of a 3/2 switched-reluctance machine.

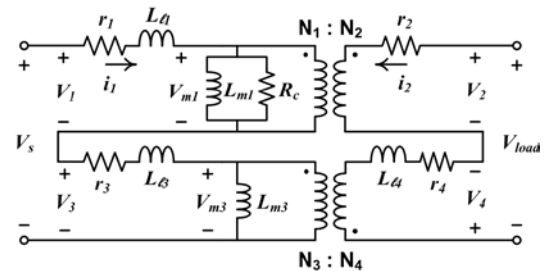


Fig. 3. Equivalent circuit for the emulated Epstein Frame test.

of magnetic steels by the equivalent mutual inductance  $L_{mj}$  in the circuit [9]-[11], the one based on Preisach model is selected for implementation. Hence, from the converged flux information  $\phi_{mj}$  at every individual region  $j$ , the corresponding voltage  $V_{mj}$  can be derived by

$$V_{mj} = d(N_1 \phi_{mj}) / dt = d\lambda_{mj} / dt, \quad (2)$$

in which  $N_1$  is the equivalent turns for the emulated Epstein Frame test. Therefore, the voltages  $V_{sj}$  at different levels and frequencies corresponding to the given flux densities at the  $j^{\text{th}}$  region can be applied, and the resultant iron losses can then be calculated from the system voltage and current information.

### III. EMULATED RESULTS

A 6/4 switched-reluctance motor (SRM) rated at 150 V, 1.0 hp, 1000 rpm, as depicted in Fig. 4 and Table I, has been selected to perform the emulation analyses. By applying the derived air-gap MMF into the MEC that can represent the air-gaps and steel cores, based on the proposed integrated iterative scheme, the final converged flux evaluation results at one rotor position by dividing the SRM into 364 regions are illustrated in Fig. 5(a), and the corresponding results obtained from detailed FEA [12] are provided in Fig. 5(b) for comparisons. With larger number of subdivided machine core regions for MEC analyses, it is clear that the proposed scheme can supply better flux distribution estimation. The evaluated hysteresis losses of the machine corresponding to Fig. 5(a) are thus provided in Table II for adequacy confirmations.

### IV. CONCLUSIONS

A systematic scheme that can integrate the iteratively solved flux densities inside an electric machine from magnetic equivalent circuits and the calculated hysteresis losses from

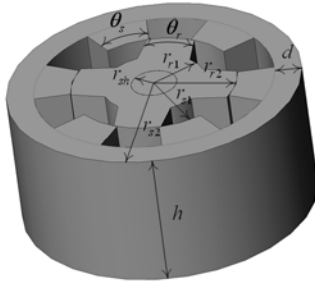
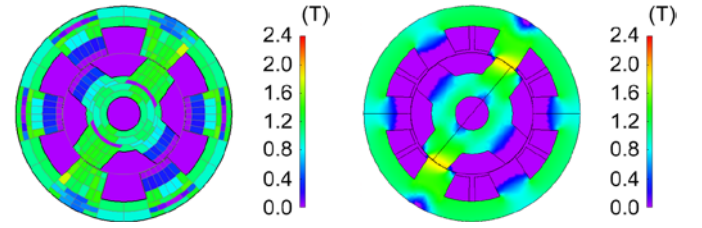


Fig. 4. Structure of a 6/4 SRM.

TABLE I  
PHYSICAL DIMENSIONS OF THE 6/4 SRM

Item	Dimension
Stator inner radius, $r_{s1}$	45.3 mm
Stator outer radius, $r_{s2}$	80.0 mm
Rotor inner radius, $r_{sh}$	12.5 mm
Rotor axial radius, $r_{r1}$	28.0 mm
Rotor outer radius, $r_{r2}$	45.0 mm
Stator yoke width, $d$	14.9 mm
Stator pole arc, $\theta_s$	30°
Rotor pole arc, $\theta_r$	32°
Stack length, $h$	75.0 mm



(a) Obtained from the proposed scheme. (b) Obtained from 3-D FEA.

Fig. 5. Flux density distributions inside the SRM at one rotor position.

TABLE II  
ESTIMATED HYSTERESIS LOSSES OF THE 6/4 SRM

From the FEA	From the Emulated Epstein Frame Tests	Difference
11.87 W	14.16 W	19.29%

emulated Epstein Frame tests is developed. The evaluated losses can properly represent those inner-loop magnetizing characteristics of machine cores without the need of applying Steimnetz's function [12] to buildup the empirical expressions. Compared with the results obtained by 3-D FEA, suitability and applicability of the proposed scheme for evaluating electric machine hysteresis losses with magnetization and space harmonics can certainly be confirmed.

### V. ACKNOWLEDGMENTS

The authors would like to express their gratitude to the financial support from the National Science Council of Taiwan under Grant No. NSC 98-2221-E-110-077-MY3.

### VI. REFERENCES

- [1] E. Dlala, "A simplified iron loss model for laminated magnetic cores," *IEEE Trans. Magn.*, vol. 44, no. 11, pp. 3169-3172, 2008.
- [2] D. Miyagi, N. Maeda, Y. Ozeki, K. Miki, and N. Takahashi, "Estimation of iron loss in motor core with shrink fitting using FEM analysis," *IEEE Trans. Magn.*, vol. 45, no. 3, pp. 1704-1707, 2009.
- [3] X. Wang, Q. Li, S. Wang, and Q. Li, "Analytical calculation of air-gap magnetic field distribution and instantaneous characteristics of brushless dc motors," *IEEE Trans. Energy Conv.*, vol. 18, no. 3, pp. 424-432, 2003.
- [4] D. Zarko, D. Ban, and T. A. Lipo, "Analytical calculation of magnetic field distribution in the slotted air gap of a surface permanent-magnet motor using complex relative air-gap permeance," *IEEE Trans. Magn.*, vol. 42, no. 7, pp. 1828-1837, 2006.
- [5] K. T. Chau, M. Cheng, and C. C. Chan, "Nonlinear magnetic circuit analysis for a novel stator doubly fed doubly salient machine," *IEEE Trans. Magn.*, vol. 38, no. 5, pp. 2382-2384, 2002.
- [6] S. D. Sudhoff, B. T. Kuhn, K. A. Corzine, and B. T. Branecky, "Magnetic equivalent circuit modeling of induction motors," *IEEE Trans. Energy Conv.*, vol. 22, no. 2, pp. 259-270, 2007.
- [7] International Standard, CEI IEC 404-2, *Methods of Measurement of the Magnetic Properties of Electrical Steel Sheet and Strip by Means of An Epstein Frame*, 1996.
- [8] ASTM Standard, A 343-97, *Standard Test Method for Alternating Current Magnetic Properties of Materials at Power Frequencies using Wattmeter-Ammeter-Voltmeter Method and 25-cm Epstein Test Frame*, 1997.
- [9] F. Preisach, "Über die magnetische nachwirkung," *Zeitschrift für Physik*, vol. 61, pp. 277-302, 1935.
- [10] D. C. Jiles and D. L. Atherton, "Ferromagnetic hysteresis," *IEEE Trans. Magn.*, vol. 19, no. 5, pp. 2183-2185, 1983.
- [11] D. L. Atherton and J. R. Beattie, "A mean field Stoner-Wohlfarth hysteresis model," *IEEE Trans. Magn.*, vol. 26, no. 6, pp. 3059-3063, 1990.
- [12] JSOL Corporation, *JMAG-Studio V10.0*, Tokyo, Japan, 2010.